

Effective-mass change of electrons in Si inversion layers under parallel magnetic fields

U. Kunze

*Institut für Elektrophysik, Technische Universität Braunschweig,
and Hochmagnetfeldanlage der Physikalischen Institute der Technischen Universität Braunschweig,
D-3300 Braunschweig, Federal Republic of Germany*

(Received 29 December 1986)

Using electron tunneling, the ground-subband wave function in a quantized electron surface layer on Si(001) is investigated under parallel magnetic fields up to $B=15$ T. A change of the effective mass of the surface electrons has been determined from the change of the energy difference $E_F - E_0$ as a function of B , where the transfer of electrons populating the low-energy tail of the $0'$ subband has been taken into account. The result is an increase of the effective mass proportional to B^2 in accordance with the prediction of second-order perturbation theory. The contribution of the ground subband to the tunneling conductance is shown to vary approximately by the same amount as the two-dimensional density of states. From the effective-mass change we obtain the spread of the wave function perpendicular to the interface. For low depletion fields the dependence of the spread on depletion charge density is reasonably described by the Fang-Howard variational wave function; at high depletion fields the experimentally determined spread is considerably lower.

I. INTRODUCTION

In a quasi-two-dimensional (quasi-2D) electron layer at the semiconductor insulator interface, a tangential magnetic field deforms the quantized wave functions perpendicular to the surface. This deformation modifies the dispersion relation of the surface subbands. At low magnetic fields, i.e., when the radius of the possible cyclotron motion is larger than the spread of the wave function, the influence of the magnetic field can be treated perturbationally. To first order, the result is a rise in the subband energy E_n (diamagnetic shift) and a displacement of the $E(\mathbf{k})$ parabola in the 2D \mathbf{k} plane perpendicular to the magnetic field direction [Fig. 1(a)], as given by¹

$$E_n(B) = E_n(0) + \frac{\hbar^2 k_y^2}{2m_y} + \frac{1}{2m_x} (\hbar k_x + eB \langle z \rangle_n)^2 + \frac{e^2 B^2}{2m_x} (\langle z^2 \rangle - \langle z \rangle_n^2), \tag{1}$$

where $\mathbf{B}=(0,B,0)$ and $(\langle z^2 \rangle - \langle z \rangle_n^2)^{1/2}$ is the spread of the wave function perpendicular to the interface at $B=0$. A second-order calculation yields the increase of the effective mass for the motion perpendicular to the magnetic field [Fig. 1(a)], which is equivalent to an increase of the 2D density of states.²⁻⁴ For electrons populating the lowest subband the effective-mass change can be written as²

$$\frac{m_x(B) - m_x(0)}{m_x(0)} = \frac{\Delta m_x}{m_x} \simeq \frac{2e^2 B^2}{m_x E_{10}} (\langle z^2 \rangle - \langle z \rangle_0^2) \tag{2}$$

with an energy separation $E_{10} = E_1 - E_0$ between the lowest and the first excited subband.

On Si(001) surfaces, the spread of the ground-state wave function is so small that usual magnetic fields up to $B=15$ T represent the low-field limit. However, the wid-

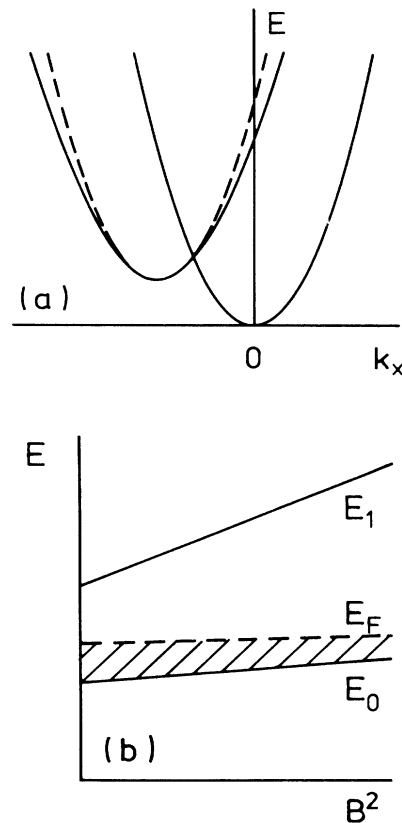


FIG. 1. (a) A parallel magnetic field B_y causes a rise in energy of the $E(k_x, k_y=0)$ parabola and a displacement along k_x (dashed curve), and reduces the curvature (solid curve). (b) Energy changes in the electron inversion layer as a function of square of magnetic field B . The diamagnetic shifts and the reduction of $E_F - E_0$ are exaggerated for clarity. The energy origin is at the bottom of the surface potential well.

er extended wave functions of higher subbands in, particularly, accumulation layers on Si (Ref. 5) or of subbands on semiconductors with small effective masses,⁴ are severely distorted by the magnetic field leading to mixed electric-magnetic surface levels.⁶ In multisubband layers these hybrid subbands must be calculated self-consistently, because the surface potential is magnetic field dependent due to redistribution of the carriers among the occupied subbands.⁷

Experimental investigations of magnetic-field-induced energy changes in 2D electron layers have been performed by means of infrared spectroscopy,^{8–13,4} magnetotransport^{14–22,7} and electron tunneling.^{23,24} Intersubband resonance energies, which have been calculated for the case of parallel²⁵ and tilted fields,²⁶ are known to give no data on the diamagnetic correction of one subband alone.⁶ In multisubband electron surface layers both the diamagnetic effect and the density-of-state increase are involved in the observed magneto-conductance oscillations¹⁵ and cannot be determined separately. Therefore the reduction in the number of occupied subbands with increasing magnetic fields has been discussed in terms of the diamagnetic rise of the subband minima neglecting the density-of-states change¹⁵ or vice versa.⁴ Other transport studies in tilted magnetic fields, where only the diamagnetic effect has been included quantitatively,²¹ may also be suspected to give incorrect results. However, tunneling spectroscopy is a unique method, which directly gives the energies of the subband minima and their shift caused by a parallel magnetic field.

The intention of Sec. II is to elucidate how the energy changes of quantized levels in the 2D surface layer can be determined by electron tunneling. Section III is concerned with the experimental results. Finally, Sec. IV briefly summarizes the conclusions.

II. REMARKS ON THE TUNNELING METHOD

In a metal-oxide-semiconductor tunnel structure with quantized electron layer at the semiconductor surface, the application of a bias voltage at the metal electrode shifts the metal Fermi level by $-eV$ relative to the semiconductor Fermi level E_F , and electrons may tunnel from occupied states of one electrode into empty states of the counterelectrode. When the bias equals $V=V_n$ so that the metal Fermi level is aligned with the bottom of the n th subband, $-eV_n=E_n-E_F$, a new tunneling channel opens for those electrons starting at the metal Fermi energy, which leads to a pronounced structure in the second derivative $d^2I/dV^2(V)$ of the current-voltage characteristic, where $dI/dV^2(V)$ denotes d^2I/dV^2 as a function of bias V . The bias position V_0 of that structure arising from the bottom of the lowest subband E_0 reflects the areal density N_0 of electrons in this subband according to

$$eV_0 = E_F - E_0 = N_0/D_0, \quad (3)$$

where D_0 is the 2D density of states.^{27,28} In the electric quantum limit N_0 is equal to the total surface electron density N_s .

When the 2D electron system is subjected to a parallel magnetic field, the subband minima are shifted to higher energies as given by Eq. (1). It should be emphasized that

this shift is a magnetic-field-induced correction of the electric subband energy measured from the *bottom of the surface potential well*. On the other hand, tunneling spectroscopy measures the subband energies *relative to the Fermi level* E_F . Hence, any change of the bias position V_0 reflects a variation of the surface density of electrons N_0 and/or of the density of states D_0 [Eq. (3)], whereas the diamagnetic rise of the ground subband in principle cannot be directly determined by tunneling. Although this interpretation disagrees with that given in Ref. 23, the numerical results presented there need not be far from true, which will be shown at the end of the discussion.

In contrast to the diamagnetic shift of the lowest subband, that of the higher subbands can be measured by tunneling with a negligibly small amount of systematic error. Compared to the ground subband, the wave functions of excited subbands are extended much deeper into the bulk, and their diamagnetic effect is more than 1 order of magnitude larger. As will be shown in the following, the change of the Fermi energy relative to the bottom of the potential well is even less than the diamagnetic shift of the ground subband. Hence the Fermi level is a good reference level for determining the diamagnetic rise of excited subbands, which can be read from the change in the bias positions V_n of the subband-edge-induced structures in d^2I/dV^2 as a function of V .²⁴

On Si(001) surfaces the lowest subband is isotropic ($m_x = m_y$) for $B = 0$. When $B > 0$ the density of states

$$D_0(B) = \frac{2}{\pi\hbar^2} (m_x m_y)^{1/2} \simeq D_0(0) \left[1 + \frac{1}{2} \frac{\Delta m_x}{m_x} \right] \quad (4)$$

increases with the square of magnetic field as given by $\Delta m_x/m_x$ in Eq. (2).⁴ In metal-oxide-semiconductor tunnel structures the sum of depletion charge density N_{depl} and surface electron density N_s , which is influenced by the work-function difference of the metal and semiconductor electrodes Φ_{ms} , depends on the surface capacitance C_s of the junction and on the applied bias V by²⁸

$$N_s + N_{\text{depl}} = C_s (\Phi_{ms} + eV) / e^2, \quad (5)$$

where Φ_{ms} can be regarded as independent of B in the field range of interest. In the electric quantum limit and for constant surface capacitance the density N_0 is constant. Then we may expect the energy changes in the 2D system to occur as illustrated in Fig. 1(b). An estimate for typical parameters of Si(001) surfaces gives energy changes of E_0 and $E_F - E_0$, according to Eq. (1) and Eqs. (2)–(4) respectively, of the order of 0.1 meV with opposite sign. Thus the decrease of $E_F - E_0$ approximately cancels the rise of E_0 , hence the variation of E_F , which indicates a change of the surface band bending, is extremely small.²⁴

III. EXPERIMENTAL RESULTS

Samples and experimental techniques used in the present study are the same as described in previously published work.^{24,28} Here we measure the low-temperature ($T = 4.2$ K) tunneling characteristics d^2I/dV^2 (as a function of V) of Ti/SiO₂/Si(001) junctions at constant paral-

lel magnetic fields up to $B=15$ T. Again, the substrate-bias technique is employed to vary the areal density N_{depl} of ionized acceptors in the depletion layer.

A. Energy change and influence of second subband occupation

Figure 2 shows typical tunneling characteristics recorded at zero magnetic field. At $B > 0$ we observe a slight shift of the bias position V_0 of the dip arising from the E_0 minimum. A reliable determination is achieved by fitting the lower part of the dip to a parabola. Owing to the low noise level at forward biases—a factor of 10 to 100 below that in the reverse-bias range²⁴—the change ΔV_0 can be determined with an uncertainty of $\pm 3 \mu\text{V}$. The result is a shift ΔV_0 proportional to B^2 up to $B=15$ T. The maximum change of V_0 at $B=15$ T amounts to -30 to $-200 \mu\text{V}$, depending on the substrate bias.

The evaluation of the energy shift according to Eqs. (3) and (4) requires an exact knowledge of the influence of the magnetic field on the electron density N_0 . An examination of the surface capacitance revealed that C_s is independent of B within the resolution of the instrument of $\Delta C_s/C_s = 5 \times 10^{-4}$, confirming a constant surface electron density N_s . We know from earlier investigations of the Si(001) electron system²⁸ that at low depletion charge densities ($N_{\text{depl}} < 4 \times 10^{11} \text{ cm}^{-2}$) a tail of states below the $E_{0'}$ minimum contains a few percent of the surface electrons even in Ti-metallized junctions of only $N_s \approx 2.5 \times 10^{12} \text{ cm}^{-2}$ electron density. Since the spread of the wave function of the $0'$ subband is larger than of the ground subband, a parallel magnetic field increases the subband separation $E_{0'} - E_0$. This results in a transfer of electrons from the $0'$ into the 0 subband leading to an increase of N_0 , which partially cancels the decrease of $E_F - E_0$ due to the density-of-states change.

For a quantitative determination of the transferred elec-

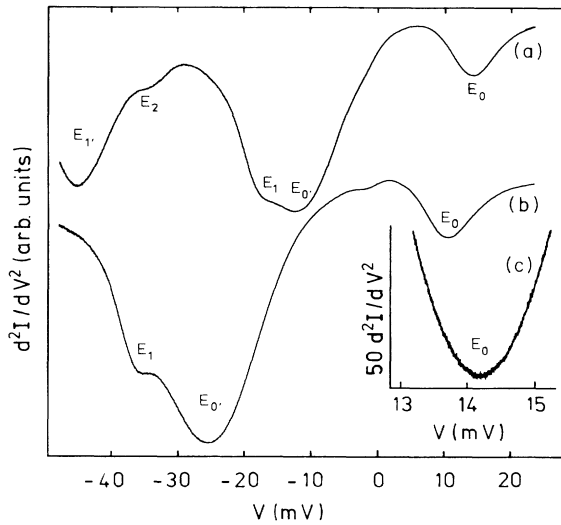


FIG. 2. $d^2I/dV^2(V)$ at $B=0$ with substrate bias (a) and (c) $V_s = -2$ V, and (b) $V_s = -20$ V. (c) is a magnified part of (a).

trons we start from the dependence of $N_{0'}$ (N_{depl}), which can be obtained from a substrate bias variation.²⁸ When N_{depl} is increased from quasiaccumulation at $V_s = +1.2$ V ($N_{\text{depl}} \approx 0.4 \times 10^{11} \text{ cm}^{-2}$) to $N_{\text{depl}} \approx 9.8 \times 10^{11} \text{ cm}^{-2}$ at $V_s = -20$ V, the density N_s reduces by the same amount [Eq. (5)], where we may neglect the simultaneous increase of C_s by less than 2%. In Fig. 3 the difference $E_F - E_0$ is plotted as a function of N_{depl} and of the reduction $\Delta N_s = -N_{\text{depl}}$ from its value $N_s \approx 2.6 \times 10^{12} \text{ cm}^{-2}$ at $N_{\text{depl}} \approx 0$. At low N_{depl} the difference $\Delta(E_F - E_0)$ between the measured curve and the asymptotic straight line reflects those electrons populating the states in a tail below $E_{0'}$, which are transferred into the 0 subband when $E_{0'}$ is raised with increasing N_{depl} . Thus their surface density is given by

$$N_{0'}(N_{\text{depl}}) = D_0 \Delta(E_F - E_0). \quad (6)$$

From this dependence we obtain the effective density of states in the low-energy tail at the Fermi level defined by

$$D_{0'}(E_F) = - \frac{\partial N_{0'}}{\partial E_{0'F}} = - \frac{\partial N_{0'}}{\partial N_{\text{depl}}} \left[\frac{\partial E_{0'F}}{\partial N_{\text{depl}}} \right]^{-1}, \quad (7)$$

where $E_{0'F} = E_{0'} - E_F$ varies linearly with N_{depl} as shown in Fig. 3. Figure 4 presents $N_{0'}$ and $D_{0'}(E_F)$ as a function of N_{depl} .

The measured variation of E_{F0} due to a parallel magnetic field, $\Delta E_{F0}(B)$, is the sum of the change $\Delta E_{F0}^{\text{DOS}}(B)$ caused by the density-of-states effect and a correction $\Delta E_{F0}^{\text{ET}}(B)$ due to electron transfer, which can be expressed according to Eq. (7) as

$$\Delta E_{F0}^{\text{ET}}(B) \approx \frac{\Delta N_0(B)}{D_0(E_F)} \approx \frac{D_{0'}(E_F)}{D_0(E_F)} \Delta E_{0'F}(B). \quad (8)$$

In

$$\Delta E_{0'F}(B) = \Delta E_{0'0}(B) - \Delta E_{F0}(B) \quad (9)$$

the term $\Delta E_{0'0}(B) = \Delta E_{0'}(B) - \Delta E_0(B)$ describes the diamagnetic shifts of the subbands $0'$ and 0 . To lowest or-

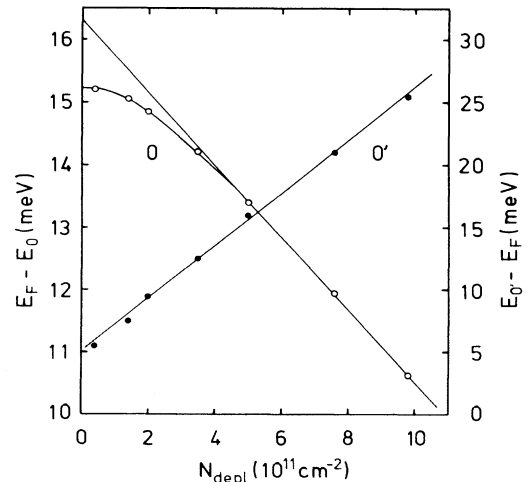


FIG. 3. $E_F - E_0$ and $E_{0'} - E_F$ as a function of N_{depl} .

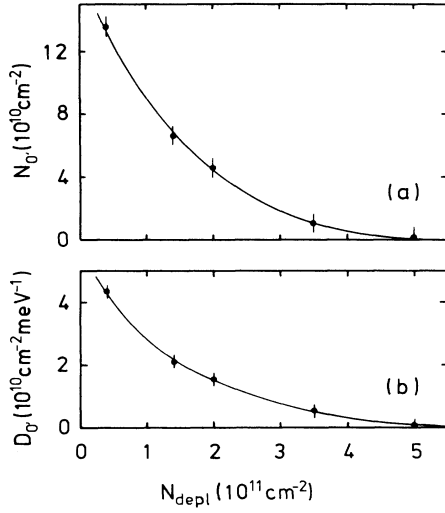


FIG. 4. (a) Electron density N_0 populating the $0'$ band tail and (b) $D_0(E)$ as defined in the text as a function of N_{depl} . Solid lines are guides for the eye.

der, ΔE_{0F} is proportional to B^2 and $D_0(E_F)$ is constant [Eq. (4), $B=0$]. Since the dependence of $\Delta E_{F0}^{\text{ET}}(B)$ on N_{depl} is mainly contained in $D_0(E_F)$, we may use a constant value for $\gamma = \partial(E_{0F})/\partial(B^2)$, where the spread of the 0 and the $0'$ subband wave functions is regarded as constant. An evaluation of $\Delta V_0(B)$ according to Eqs. (2) and (4), neglecting the correction $\Delta E_{F0}^{\text{ET}}$, yields an approximate value $(\langle z^2 \rangle - \langle z \rangle^2)_0^{1/2} \simeq 1.4 \pm 0.1 \text{ nm}$. The spread of the $0'$ wave function, gained from an extrapolation of earlier results²⁴ on the subbands $1'-5'$, amounts to $2.5 \pm 0.3 \text{ nm}$. The resulting constant $\gamma = 1.7 \pm 0.5 \mu\text{eV T}^{-2}$ leads to a correction $\Delta E_{F0}^{\text{ET}}(B)$ of about 20% of the measured variation $\Delta E_{F0}(B)$ at $N_{\text{depl}} = 2.0 \times 10^{11} \text{ cm}^{-2}$ ($V_s = 0$). Figure 5 shows the corrected energy shift $\Delta E_{F0}^{\text{DOS}}(B)$. The right-hand scale for $\Delta m_x/m_x(B)$, calculated from Eqs. (2) and (4), gives an increase of the effective mass of less than

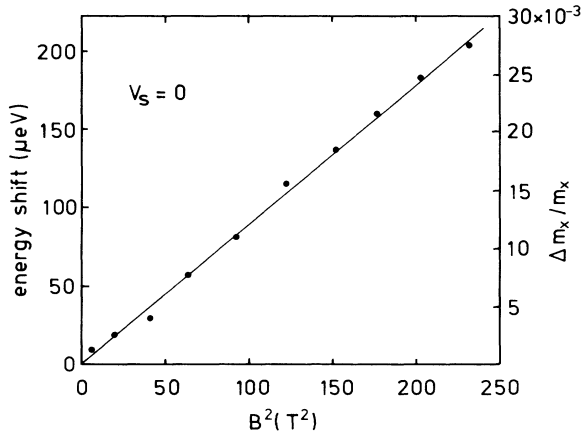


FIG. 5. Energy shift $\Delta E_{F0}^{\text{DOS}}$ and effective-mass change as a function of B^2 ($V_s = 0$). The solid straight line is a fit to the experimental points.

3%, i.e., the constant-energy line is deformed from a circle into an ellipse by stretching the main axis along k_x by less than 1.5%.

B. Tunneling conductance in parallel magnetic fields

The deformation of the wave function should result in a change of the probability for tunneling of the surface electrons into the metal electrode. (It is obvious that the same is true for tunneling in the reverse direction or into higher subbands, which we are not concerned with.) Provided that this change mainly arises from the change of the 2D density of states $D_0(B)$ to which the contribution g_0 of the ground subband to the tunneling conductance $g = dI/dV$ is proportional,²⁹ we have a second experimental way of determining $D_0(B)$. Owing to the steplike character of the conductance dI/dV at positive biases around $V = V_0$,^{28,30} we obtain the contribution g_0 from the difference between the conductance at biases $V_a < V_0$ and $V_b > V_0$, where V_0 is N_{depl} dependent as shown in Fig. 3. For all values of N_{depl} , any influence of the conductance decreases due to E_0 and $E_{0'}$ as well as of the magnetic-field-dependent zero-bias anomaly could be avoided when V_a is chosen in a range of 4.5–5.5 mV. In a bias range $25 \leq V_b \leq 45 \text{ mV}$, well below the phonon threshold at $V = 50 \text{ mV}$,²⁸ the background conductance is nearly constant and not affected by the magnetic field. We used $V_a = 5 \text{ mV}$ and $V_b = 35 \text{ mV}$ for the measurement of $\Delta g_0(B) = g_0(B) - g_0(0)$, where $g_0 = g(V_a) - g(V_b)$.

The resulting plot in Fig. 6 reveals the same variation of $\Delta g_0/g_0$ with respect to B^2 as expected from the density of states in Eq. (4) and the effective-mass change shown in Fig. 5. Hence we may express the conductance change in terms of the effective-mass change according to $\Delta g_0/g_0 \simeq \Delta D_0/D_0 \simeq \Delta m_x/2m_x$. However, at high depletion fields $\Delta g_0/g_0$ exhibits a somewhat larger variation than $\Delta D_0/D_0$, which indicates an increase of the tunneling probability beyond the density-of-states effect.

C. Spread of the ground-state wave function

Using Eq. (2) we have determined the dependence of the spread $(\langle z^2 \rangle - \langle z \rangle^2)^{1/2}$ of the ground-state wave function

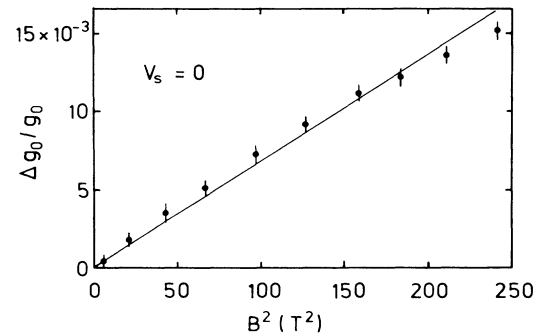


FIG. 6. Relative change of the contribution g_0 of the lowest subband to the tunneling conductance as a function of B^2 ($V_s = 0$). The solid straight line is a fit to the experimental points.

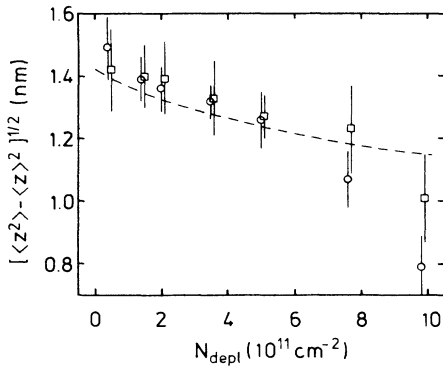


FIG. 7. Spread of the ground-subband wave function as a function of depletion charge density N_{depl} . Experimental points are obtained from the effective-mass change (circles) and from the conductance change (squares). The dashed line represents the result of the Fang-Howard variational function (see text).

on the depletion charge density (Fig. 7), where the subband separation $E_1 - E_0$ has been directly obtained from the tunneling characteristics as shown in Fig. 2. It should be noted once more that while increasing the depletion charge density N_{depl} the surface electron density decreases from 2.6×10^{12} to 1.7×10^{12} cm^{-2} as illustrated by Fig. 3 and Eq. (5). The data points from the conductance change are also included into the diagram. However, it follows from the discussion in Sec. III B that at high depletion charge densities, where the results obtained from both measurements are different, those data gained from the energy change are more reliable.

Particularly at low N_{depl} the experimental results are reasonably described by the dashed line calculated from the variational function^{1,31}

$$\zeta_0(z) = \left(\frac{1}{2}b^3\right)^{1/2} z \exp(-bz/2), \quad (10)$$

where in the variational parameter b given by ($m_z = 0.916 m_0$)

$$b^3 \simeq \frac{12m_z e^2}{\epsilon_0 \epsilon_{\text{Si}} \hbar^2} (N_{\text{depl}} + \frac{11}{32} N_0) \quad (11)$$

the electron density N_0 depends on N_{depl} as shown in Fig. 3. The spread of the variational function is $1/b$.

At high N_{depl} the experimental points clearly deviate from the theoretical curve. This arises probably from too slow a decay of the variational wave function into the semiconductor electrode. With increasing depletion field and decreasing surface field (N_0 reduces) the surface potential well is approaching the triangular form. Hence the asymptotic behavior of the subband wave function is closer to $\exp(-z^{3/2})$ of the Airy function than to $\exp(-z)$ of the variational function.

Finally, we return to the question of how much the energy shift $\Delta E_{F0}(B)$ differs from the diamagnetic rise $\Delta E_0(B)$. Using the experimentally determined spread of the wave functions, we obtain the following energy changes at $B=10$ T for various N_{depl} : $N_{\text{depl}}=0.4 \times 10^{11}$ cm^{-2} , $|\Delta E_{F0}|=127 \pm 12$ μeV , $\Delta E_0=103 \pm 14$ μeV ; $N_{\text{depl}}=2.0 \times 10^{11}$ cm^{-2} , $|\Delta E_{F0}|=90 \pm 7$ μeV , $\Delta E_0=86 \pm 9$ μeV ; $N_{\text{depl}}=9.8 \times 10^{11}$ cm^{-2} , $|\Delta E_{F0}|=13 \pm 2$ μeV , $\Delta E_0=29 \pm 7$ μeV . These values show clearly that except for high depletion fields both energy changes are nearly equal.

IV. CONCLUSIONS

The change of the effective mass of surface electrons in a parallel magnetic field leads to an increase of the 2D density of states. This increase results in a change of the difference $E_F - E_0$, which we have directly obtained from the tunneling characteristics of a metal-SiO₂-inverted p -type Si structure. In contrast to this energy change, the diamagnetic rise of the ground subband is in principle undetectable by tunneling.

In evaluating the energy shift we have taken into account those electrons, which particularly at low depletion fields populate a low-energy tail of the O' subband, and which become transferred into the lowest subband when the magnetic field increases the subband energy $E_{O'}$ relative to E_F . The resulting effective-mass change is of the order of 1% at $B=15$ T, which is probably too small to be measured by any other experimental technique.

The influence of the parallel field on the tunneling probability is studied from the change in the contribution of the lowest subband to the tunneling conductance. When the depletion field is much less than the surface field, the conductance change is approximately the same as the density-of-states change. At high depletion fields the conductance varies somewhat stronger with magnetic field than the density of states.

Since tunneling characteristics directly give the subband separation, we are able to determine the spread of the ground-state wave function from the effective-mass change, where we apply the result of a second-order perturbational calculation. At low depletion fields the dependence of the spread on N_{depl} is reasonably described by the Fang-Howard variational function. The failure of the theoretical model to reproduce the strong decrease of the spread obtained at high depletion fields is probably due to too slow a decay of the variational wave function into the bulk.

ACKNOWLEDGMENTS

The author thanks Professor G. Lantz for continuous encouragement and Professor U. Merkt for stimulating discussions.

¹F. Stern and W. E. Howard, Phys. Rev. **163**, 816 (1967);

²F. Stern, Phys. Rev. Lett. **21**, 1687 (1968).

³Y. Uemura, in *Proceedings of the Twelfth International Conference on the Physics of Semiconductors, Stuttgart, 1974*, edited

by M. H. Pilkuhn (Teubner, Stuttgart, 1974), p. 665.

⁴U. Merkt, Phys. Rev. B **32**, 6699 (1985).

⁵T. Ando, J. Phys. Soc. Jpn. **39**, 411 (1975).

⁶F. Koch, in *Physics in High Magnetic Fields*, edited by S. Chi-

- kazumi and N. Miura (Springer, Berlin, 1981), p. 262.
- ⁷H. Reisinger and F. Koch, *Surf. Sci.* **170**, 397 (1986).
- ⁸C. L. Zipfel, T. R. Brown, and C. C. Grimes, *Surf. Sci.* **58**, 283 (1976).
- ⁹W. Beinvogl, A. Kamgar, and J. F. Koch, *Phys. Rev. B* **14**, 4274 (1976).
- ¹⁰W. Beinvogl and J. F. Koch, *Phys. Rev. Lett.* **40**, 1736 (1978).
- ¹¹J. C. Maan, Ch. Uihlein, L. L. Chang, and L. Esaki, *Solid State Commun.* **44**, 653 (1982).
- ¹²J. H. Crasemann, U. Merkt, and J. P. Kotthaus, *Phys. Rev. B* **28**, 2271 (1983).
- ¹³S. Oelting, U. Merkt, and J. P. Kotthaus, *Surf. Sci.* **170**, 402 (1986).
- ¹⁴S. Tansal, A. B. Fowler, and R. F. Cotellessa, *Phys. Rev.* **178**, 1326 (1969).
- ¹⁵R. E. Doezema, M. Nealon, and S. Whitmore, *Phys. Rev. Lett.* **45**, 1593 (1980).
- ¹⁶M. Dealon, S. Whitmore, R. R. Bourassa, and R. E. Doezema, *Surf. Sci.* **113**, 282 (1982).
- ¹⁷M. Nealon and R. E. Doezema, *Solid State Commun.* **50**, 661 (1984).
- ¹⁸J. C. Portal, R. J. Nicholas, M. A. Brummel, A. Y. Cho, K. Y. Cheng, and T. P. Pearsall, *Solid State Commun.* **43**, 907 (1982).
- ¹⁹Th. Englert, J. C. Maan, D. C. Tsui, and A. C. Gossard, *Solid State Commun.* **45**, 989 (1983).
- ²⁰W. Zhao, F. Koch, J. Ziegler, and H. Maier, *Phys. Rev. B* **31**, 2416 (1985).
- ²¹E. J. Pakulis, *Phys. Rev. B* **31**, 6807 (1985).
- ²²A. Zrenner, H. Reisinger, F. Koch, K. Ploog, and J. C. Maan, *Phys. Rev. B* **33**, 5607 (1986).
- ²³D. C. Tsui, *Solid State Commun.* **9**, 1789 (1971).
- ²⁴U. Kunze, *Surf. Sci.* **170**, 353 (1986).
- ²⁵T. Ando, *J. Phys. Soc. Jpn.* **44**, 475 (1978).
- ²⁶T. Ando, *Phys. Rev. B* **19**, 2106 (1979).
- ²⁷D. C. Tsui, *Phys. Rev. B* **4**, 4438 (1971).
- ²⁸U. Kunze, *J. Phys. C* **17**, 5677 (1984).
- ²⁹D. J. BenDaniel and C. B. Duke, *Phys. Rev.* **160**, 679 (1967).
- ³⁰U. Kunze and G. Lautz, *Surf. Sci.* **113**, 55 (1982).
- ³¹F. F. Fang and W. E. Howard, *Phys. Rev. Lett.* **16**, 797 (1966).